Appl Water Sci (2015) 5:271–282
DOI 10.1007/s13201-014-0188-4

ORIGINAL ARTICLE

Neural network model and isotherm study for removal of phenol from aqueous solution by orange peel ash

Naba Kumar Mondal · Ria Bhaumik · Biswajit Das · Palas Roy · Jayanta Kumar Datta · Siddhartha Bhattacharyya · Siddhartha Bhattacharjee

Received: 12 January 2014 / Accepted: 1 April 2014 / Published online: 24 April 2014

Abstract Artificial Neural Network model and isotherm study were done to predict the removal efficiency of phenol. An inexpensive adsorbent was developed from orange peel ash (OPA) for effective uptake of phenol from aqueous solution. The influence of different experimental parameters (initial concentration, pH, adsorbents dose, contact time, stirring rate and temperature) on phenol uptake efficiency was evaluated. Phenol was adsorbed by the OPA up to maximum of 97.34 %. Adsorption of phenol on OPA correlated well with the Langmuir isotherm model, implying monolayer coverage of phenol onto the surface of the adsorbent. The maximum adsorption capacity was found to be 3.55 mg g^{-1} at 303 K. Pseudo-second-order kinetic model provided a better correlation for the experimental data. Moreover, the activation energy of the adsorption process (E_a) was found to be -18.001 kJ mol^{-1} indicating physorption nature of phenol onto OPA. A negative enthalpy ($\Delta H°$) value indicated that the adsorption process was exothermic. Again multi-layer Neural Network model was in very good agreement with the experimental results.

Keywords Phenol · Orange peel ash · Isotherm model · Kinetics · Physorption · ANN model

N. K. Mondal (✉) · R. Bhaumik · B. Das · P. Roy · J. K. Datta
Department of Environmental Science, The University of Burdwan, Burdwan, West Bengal, India
e-mail: nkmenvbu@gmail.com

S. Bhattacharyya
RCC Institute of Information Technology, Canal South Road, Kolkata 700015, India

S. Bhattacharjee
Tata Consultancy Services, Kolkata, India

Introduction

Phenols and its derivatives such as chloro and nitro phenols are toxic and carcinogen, usually present in industrial waste water. Very small concentration of phenol may cause vomiting, anorexia, liver and kidney damage, fainting and even mental disturbance. Phenols, long term affecting pollutants can be found in industries which produce chlorophenols that are widely used as fungicides and insecticides in agricultural sector. Phenolic compounds in potable water at the low level of 5 μg/L emit an unpleasant odor and flavor and considered poisonous to aquatic life, plants and human. Ingestion of phenols through water in concentration from 10 to 240 mg L^{-1} for a long time causes mouth irritation, diarrhea, and excretion of dark urine and vision problems (Hegazy et al. 2013; Asma and Zainal 2009). The WHO (2008) recommended threshold limit of phenol in potable water as 0.001 mg L^{-1} (Zeng et al. 2009), while US Environmental Protection Agency (EPA) recommended the permissible limit of phenols in the wastewater <1 mg L^{-1} (Eahart et al. 1977). Phenols can be removed from the aqueous solution through oxidation, precipitation, ion exchange, biodegradation, ultrasonic degradation, solvent extraction, ozonization and decomposition by fenton reagent (Aksu and Yener 2001; Rengaraj et al. 2002). Adsorption is a well-established, low cost and powerful technique for treating domestic and industrial effluents. Recent literature highlighted the extensive use of activated carbon in the field of wastewater treatment (Lotfy et al. 2012; Olafadehan et al. 2012). However, Many other adsorbents like bottom ash, brick-kilm ash, fly ash, peat, soil, rice husk, wood, saw dust, bagasse and carbonized bark are extensively used for removal of organic pollutants (Ademiluy et al. 2009; Aksu and Yener 2001; Hamza et al. 2012; Rengaraj et al. 2002).

For fine tuning and predicting the adsorption mechanism, many software-based models have been used (Carsky and Do 1999; Cuco et al. 2009). In recent years, ANN has become a popular choice among engineers and scientists as one of the powerful tools for predicting contamination and concentration of different effluents and chemicals in drinking water, wastewater and aquifers and energy content in municipal solid waste (Ogwueleka and Ogwueleka 2010). ANN model was used by Bhattacharjya et al. (2007) and Chelani et al. (2004) to characterize the salt water in a coastal aquifer and comparison was made between ANN and multivariate regression.

Orange, as a kind of biological resources, is available in large quantities in many parts of the world (Shan et al. 2012). As the orange residue, orange peel mainly consists of cellulose, hemi-cellulose and lignin in the form of carboxyl and hydroxyl, which results in high affinity to both inorganic and organic moiety. Although many studies in literatures have focused on the modification of orange waste by common chemical modifications such as alkaline and acid treatment, the adsorption capacity and selectivity of heavy metal ions on orange waste are well-documented (Ning-chuan and Xue-yi, 2012; Shan et al. 2012; Li et al. 2007). But removal of organic pollutant using OPA is very limited. In the present study, a simple and economic preparation of the adsorbent from orange peel was performed and adsorption experiments were conducted for removal of phenol from aqueous medium. The equilibrium isotherm data were fitted in Langmuir, Freundlich and DR and Temkin equations. Adsorption kinetics of phenol onto OPA was also studied using kinetic models. Finally the experimental results were analyzed with the help of neural network model.

Materials and methods

Preparation of OPA

Orange peel was collected from fruit juice shop of local market and thoroughly washed with distilled water. Orange peels were dried up in an oven at 80 °C for overnight, cut into small pieces and then carbonized into muffle furnace at 540 ± 2 °C for 1 h. The orange peel ash (OPA) was ground well into a fine powder with a mortar and pestle and sieved through a 250 μm and stored for further use.

Reagents and experimental procedure

A stock solution of phenol was prepared by dissolving 0.5 g of phenol (E. Merck Ltd., India) in double-distilled water in a 500 mL volumetric flask. This was treated as stock solution of phenol with a strength of 1,000 ppm. All the intermediate phenolic solution of lower strength was prepared from this stock solution. About 1.0 g of powder was taken into a 250 cm^3 conical flask for batch adsorption process. The pH of the solution was adjusted to the required level, using either HCl (0.1 mol/L) or NaOH (0.1 mol/L) solutions whenever necessary.

Adsorption experiments

Batch adsorption study for different experimental variables (pH; initial concentration; adsorbent dose; stirring rate; contact time and temperature) was carried out by agitating 2.0 g of OPA with 100 mL of synthetic phenol solution in 500 mL conical flask in a temperature-controlled magnetic stirrer (BZMS448 REMI Equipments; Pvt. Ltd., Mumbai, India). At the end of predetermined time interval, the content was filtered and the supernatant was analyzed for residual concentration of phenol spectrophotometrically (APHA et al. 1995) using UV–visible spectrophotometer (Systronics, Vis double beem Spectro 1203).

The amount of phenol adsorbed at equilibrium, q_e (mgg^{-1}) was determined using the following equation:

$$q_e = \frac{(C_i - C_f)V}{m} \quad (1)$$

where, V = Volume (L) of the equilibrated solution
m = Mass of used OPA (g)
C_i = Initial concentration of phenol (mg L^{-1})
C_f = Equilibrium concentration of phenol (mg L^{-1})

Artificial neural network model

ANN model is a mathematical model made up of simple processing units, which may store experimental data and make it available for further use. The sorption efficiency of OPA was calculated using mathematical software (Neural Network Toolbox Neuro Solution 5 ®). Twenty-four experimental sets were used to develop the ANN model. A multi-layer ANN with sigmoid axon transfer function was used for input and output layers. The data generated from batch experiments and same was used for input and desired matrix. The trained ANN model output results were tested with the experimental output results of phenol adsorption on OPA. The training of the ANN model was done with six neurons in the hidden layer.

Multi-layer perceptron

A typical multi-layer perception is a feed forward ANN model that maps sets onto a set of appropriate outputs. It can learn examples that are "non-linearly separable" like the XOR problem. An additional layer referred to as the

'hidden layer' is present between the input and the output layer to handle the non-linearity problem. The number of nodes in the input layer is depended upon the number of variable input parameters in the training dataset. In this present study the same number of nodes was used in the hidden layer as in the input layer for better training.

Back propagation algorithm

The teaching of ANN model was done by back propagation. This algorithm of adjusting the weights of the different network layers starting from the output layer and proceeding downstream is referred to the back propagation algorithm. It was basically worked on the basis of delta rule and required a data set of the desired output for many inputs. Moreover, it is very useful for feed forward network.

Procedure

The net inputs to the network as

$$A(x,w) = \sum_{i=0}^{n} x_i w_{ji} + \theta \tag{2}$$

where x_i= inputs, w_{ji}= weights of connection, θ=threshold = 0.5 (this value was taken because the input data comprises between 0 and 1.)

Then the output was computed by the application of the sigmoid activation function as

$$O_j(x,w) = \frac{1}{1+e^{A_j(x,w)}} \tag{3}$$

The system error was given by

$$E(x,w,d) = \sum_{j} \left(O_j(x,w) - d_j\right)^2 \tag{4}$$

where d_j= actual output

Finally the interconnection weights are adjusted using the backpropagation algorithm as

$$\Delta v_{ik} = -\eta\left(\frac{\partial E}{\partial v_{ik}}\right) = -\eta\left(\frac{\partial E}{\partial x_i} \times \frac{\partial x_i}{\partial v_{ik}}\right) \tag{5}$$

where

$$\frac{\partial E}{\partial w_{ji}} = 2(O_j - d_j)O_j(1-O_j)w_{ji} \tag{6}$$

and

$$\frac{\partial x_i}{\partial v_{ik}} = x_i(1-x_i)v_{ik} \tag{7}$$

where,v_{ik} = weights of hidden layer η = momentum, the value of μ was taken to be 0.02

Mean square error (MSE)

The MSE values were calculated by the following equation

$$\text{MSE} = \frac{1}{N}\sum\sum_{i=1} N(T_i - A_i) \tag{8}$$

where, N = number of data point
T_i = Network predicted value at the ith data
A_i = Experimental value at the ith data
i = an index of the data.

The multi-layer perception model was used for prediction of phenol removal and backpropagation algorithm was used to train the Neural Network (Fig. 1).

Results and discussion

Adsorbent characteristics

The OPA behaves as neutral at pH zero change. The results are shown in Fig. 2. The physicochemical properties of OPA are summarized in Table 1. To identify the functional

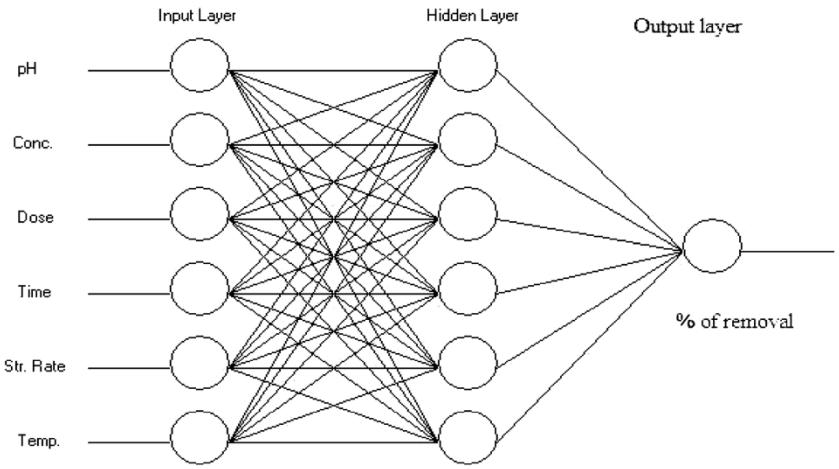

Fig. 1 Neural network architecture

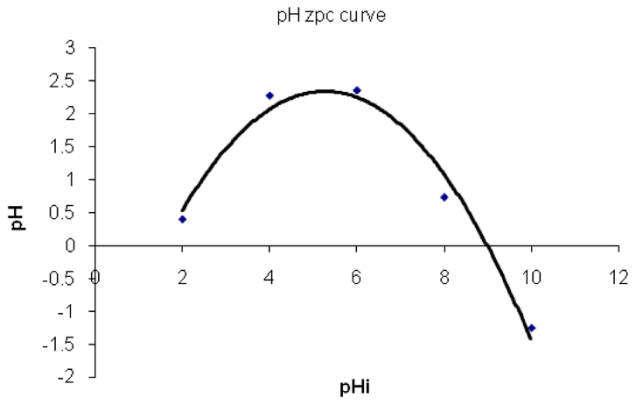

Fig. 2 Plot of ΔpH vs. pH_i

Table 1 Physico-chemical properties of OPA

Parameters	Value
pH	7.8
pH_{zpc}	9.1
Moisture content (%)	2.16
Specific gravity	0.29
Bulk density (g cm^{-3})	0.26
Particle density (g cm^{-3})	0.35
Porosity (%)	25.92
Particle size (μm)	250
Surface area (m^2g^{-1})	141
Ash content (%)	3.6

groups available on the surface of the investigated adsorbents, the IR spectra were recorded as shown in the Fig. 3a, b. Before adsorption of fluoride OPA showed intense bands at 3,418.60, 2,345.42, 2,363.97, 1,420.20 cm^{-1} and 1,048.22 cm^{-1}. Among these, the bands at 3,418.60 cm^{-1} and 1,420.20 cm^{-1} are attributed to the hydroxyl and amino groups, respectively. But the peak at 3,418.60 cm^{-1} was shifted to the 3,443.98 cm^{-1} and the peak at 1,420.20 cm^{-1} splitted to 1,625 cm^{-1} and 1,437 cm^{-1}. This is probably due to the interaction between −OH and $-NH_2$ functional groups of adsorbents and phenoxide ions. Characterization of the OPA (before and after adsorption) was also done using SEM micrograph shown in Fig. 4a, b. It is evident from the micrograph that OPA powder was an assemblage of fine particles, which did not have regular fixed shape and size. But after passing phenol solution, adsorbent surface showed uneven surface texture along with lot of irregular surface.

Effect of pH

The initial pH of adsorption medium is one of the most important parameters affecting the adsorption process. The adsorption of phenol by OPA was studied at various pH ranging from 3.0 to 7.0 (Fig. 5). It is revealed that the adsorption of phenol by OPA was highest at pH 5.0 and thereafter adsorption was decreased with increasing pH of the medium. It seems to be possible because the surface behaves as positive when $pH < pH_{zpc}$ and adsorption of anion is favored while adsorption of cation is favorable when $pH > pH_{zpc}$ (Gholami et al. 2006). The ionic fraction of phenolate ion (ionsφ) can be calculated from the following equation (Banat et al. 2000):

$$\phi_{ions} = 1/1 + 10_{a}^{PK} - pH \quad (9)$$

At low pH, the surface of the OPA is usually protonated and resulted in a stronger attraction for the negatively charged phenolate ions. This is also justified by the pH_{zpc} value (9.1); because maximum adsorption occurs at pH 5 which is just below the pH_{zpc} value. Phenol, being weakly acidic ($pKa = 10$), partially ionizes in solution and transformed to negatively charged and is directly attracted to the protonated surface of OPA by electro-static force. Unionized phenol molecules would also be attracted, possibly, by physical force. Non-ionized phenol molecules would also be attracted, possibly, by physical force. At high pH, OH^- ions would compete with the phenolate ions for sorption sites. Sorption of excess of OH^- ions could create a negative charge on the OPA surface resulting repulsion of negatively charged phenoxide ions, and therefore, adsorption is decreased (Uddin et al. 2007). The experimental data and ANN-calculated outputs are compared with ANN model and shows a good performance in the prediction of the experimental data (Fig. 11a).

Effect of adsorbent dosage

To investigate the effect of mass of adsorbent on the adsorption of phenol, a series of adsorption experiments were carried out with different adsorbent dosages at an initial phenol concentration of 50 mg L^{-1}. Fig. 6 shows the effect of adsorbent dosage on the adsorption of phenol. The percentage removal of phenol increased with the increasing absorbent dosage (0.5–4.0 g). It is attributed due to increase in adsorbent surface area and availability of more adsorption sites (Mehrizad et al. 2009; Uddin et al. 2007). The results also revealed that the adsorption efficiency increases with the increasing dose (Rengaraj et al. 2002). The experimental output data are well-fitted with the ANN output data.

Effect of stirring rate

The effect of stirring rate on the adsorption of phenol is shown in Fig. 7. There is a steady increase in the

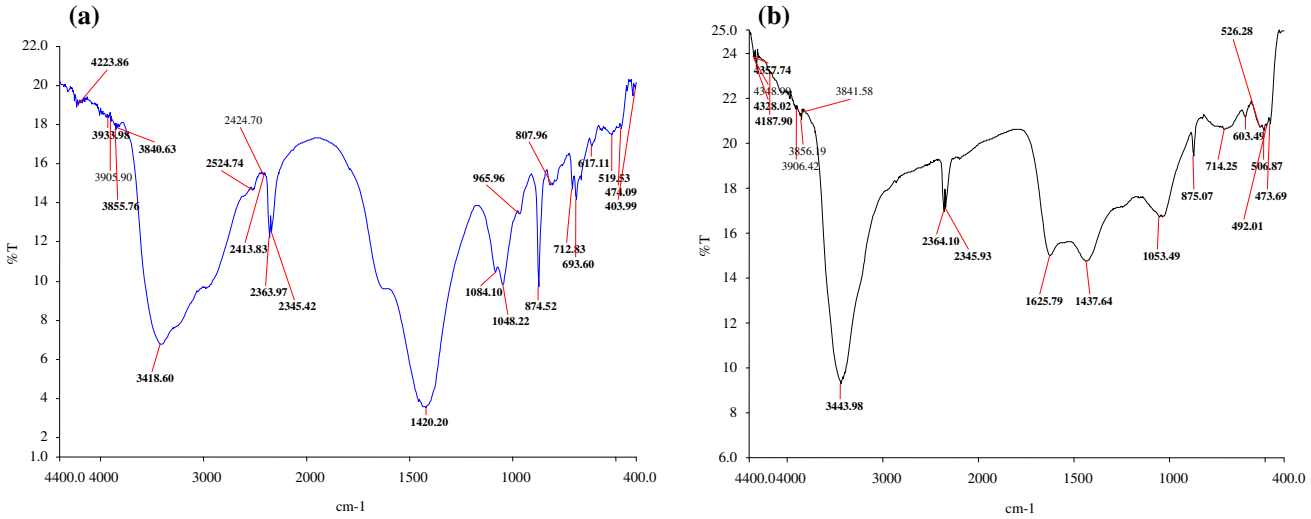

Fig. 3 **a** FTIR spectra of OPA before phenol adsorption. **b** FTIR spectra of OPA after phenol adsorption

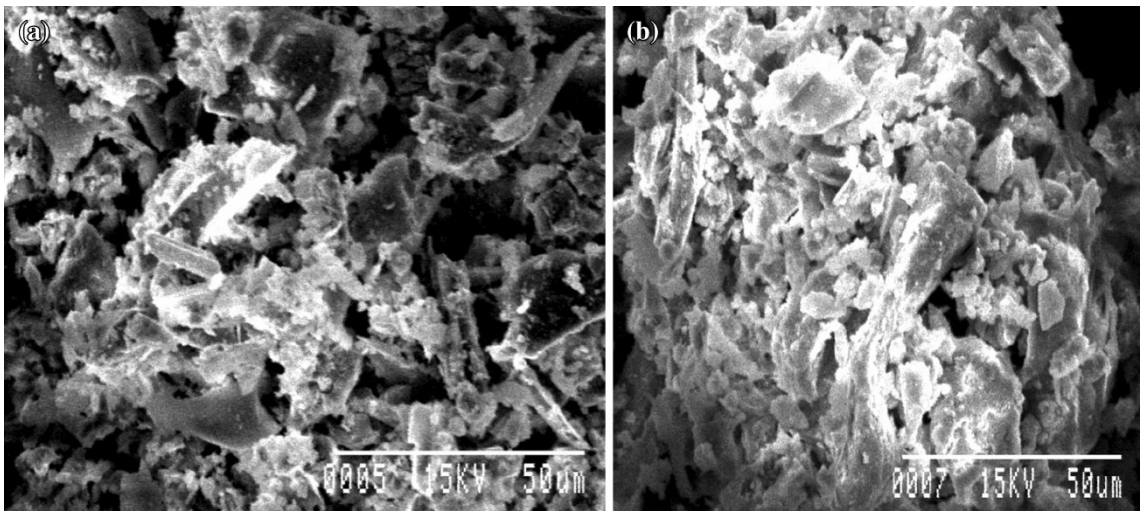

Fig. 4 **a** SEM of OPA before phenol adsorption. **b** SEM of OPA before phenol adsorption

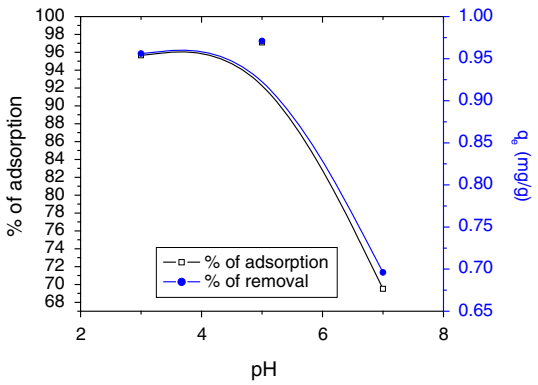

Fig. 5 Effect of pH on adsorption of Phenol using OPA (Initial Phenol concentration of 20.0 mg L^{-1}; adsorbent dose of 2.0 g/100 mL; stirring rate 150 rpm; contact time of 60 min; temperature 25 °C)

percentage of adsorption with increase in the stirring rate from 100 to 150 rpm. The maximum adsorption occurs at stirring rate of 150 rpm, and thereafter, the adsorption is almost constant. The increase in adsorption at higher stirring probably due to proper contact between the phenolate ions and the adsorbent binding sites and consequently promoting effective transfer of sorbate ions to the sorbent sites. ANN model prediction is found to be matched with the experimental data (Fig. 11d).

Effect of initial phenol concentration

The effect of initial concentration on adsorption of phenol is shown in Fig. 8. Maximum adsorption is observed for an initial concentration of 20 mg L^{-1}. Adsorption efficiency shows a decreasing trend with an increasing

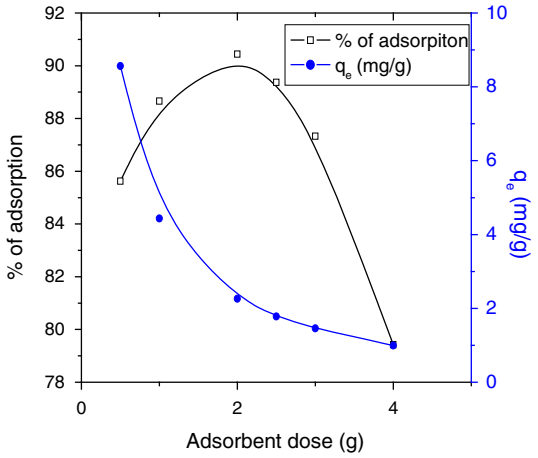

Fig. 6 Effect of adsorbent dose on adsorption of phenol using OPA (Initial Phenol concentration of 20.0 mg L^{-1}; pH 5.0; stirring rate 150 rpm; contact time of 60 min; temperature 25 °C)

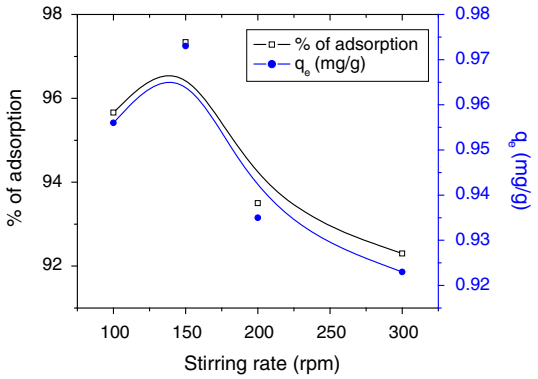

Fig. 7 Effect of stirring rate on adsorption of phenol using OPA (Initial Phenol concentration of 20.0 mg L^{-1}; pH 5.0; adsorbent dose 2.0 g; contact time 60 min; temperature 25 °C)

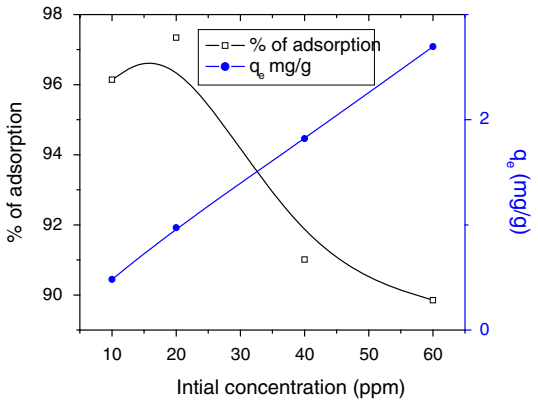

Fig. 8 Effect of Initial concentration on adsorption of phenol using OPA. (pH—5.0; adsorbent dose 2.0 g; stirring rate 150 rpm; contact time 60 min; temperature 25 °C)

concentration of phenol from 30 to 60 mg L^{-1}. It is also evident that the adsorption capacity of the sorbent is increased with the increasing phenol concentration while

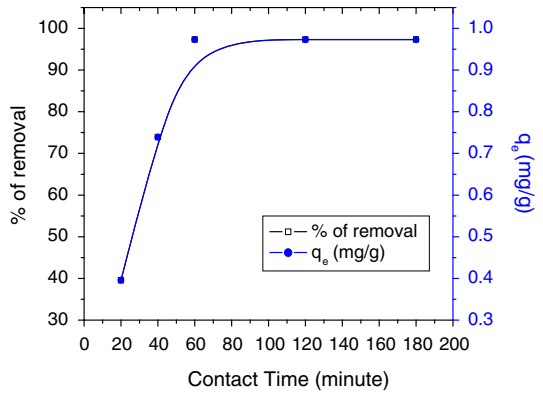

Fig. 9 Effect of contact time on adsorption of phenol using OPA (Initial concentration 20.0 mg L^{-1}; pH 5.0; adsorbent dose 2.0 g; stirring rate 150 rpm; temperature 25 °C)

the adsorption yields of phenol showed the opposite trend. It is probably due to increase in mass transfer driving force and therefore the rate at which phenol molecules pass from the bulk solution to the particle surface (Caturla et al. 1998; Imagawa et al. 2000). The experimental data and ANN-calculated output is found to be nicely matched (Fig. 11b).

Effect of contact time

The adsorption data for the uptake of phenol versus contact time is presented in Fig. 9. This result indicates that up to 90–95 % of the total phenol uptake occurs in the first rapid phase (60 min) and thereafter the adsorption rate is decreased. The higher adsorption rate at the initial period (first 40 min) may be due to large number of vacant sites on the adsorbent and as a result there exist increased concentration gradients between adsorbate in solution and adsorbate on adsorbent surface (Uddin et al. 2007). ANN model prediction in accordance with the experimental data (Fig. 11e).

Effect of temperature

Batch adsorption experiments were carried out at different temperatures ranging from 298 to 313 K (Fig. 10). It is found that with an increase in temperature from 298 to 313 K, the adsorption capacity of phenol onto OPA is decreased from 0.973 to 0.773 mgg^{-1}. The decrease of adsorption capacity at higher temperature indicates that lower temperature favors the phenol adsorption onto OPA and the adsorption is an exothermic process. At higher temperature entropy of the adsorbed molecule is probably increased and subsequently escapes from the solid adsorbent surface to the bulk phase of solution (Bhatti et al. 2010). The experimental data are fitted well with the ANN model (Fig. 11f; Table 2).

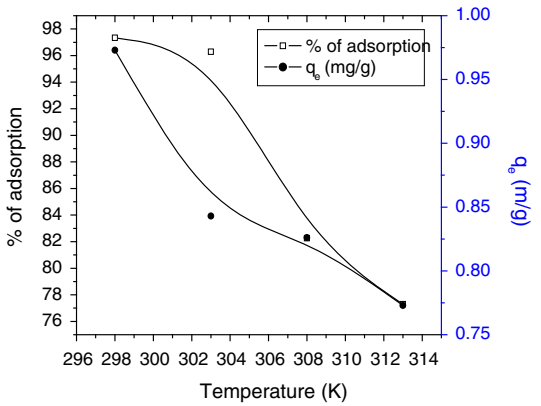

Fig. 10 Effect of temperature (K) on adsorption of phenol using OPA (Initial concentration 20.0mgL^{-1}; pH—5.0; adsorbent dose 2.0 g; Stirring rate 150 rpm; contact time 60 min.)

Adsorption isotherm

Equilibrium study provides information on the efficiency of the adsorbent. An adsorption isotherm is usually characterized by certain constant values, which express the surface properties and affinity of the adsorbent. The most widely used isotherm equations for modeling of the adsorption of phenol are as follows:

$$\frac{1}{q_e} = \frac{1}{K_L q_m}\frac{1}{C_e} + \frac{1}{q_m} \tag{10}$$

$$\log q_e = \log K_f + \frac{1}{n}\log C_e \tag{11}$$

$$q_e = q_{DR}\exp(-K_{DR}^{\varepsilon^2}) \tag{12}$$

$$q_e = B\ln K_T + B\ln C_e \tag{13}$$

where q_{max} (mgg^{-1}) and K_L (L mg^{-1}) are Langmuir parameters related to maximum adsorption capacity and free energy of adsorption, respectively. K_F and n are the Freundlich constants that indicate adsorption capacity and adsorption intensity, respectively. RT/$b_T = B$, where T is the temperature (K), and R is the ideal gas constant (8.315 Jmol^{-1}K^{-1}) and K_T (L min^{-1}) and b_T are constants. q_m (mgg^{-1}) is related to maximum adsorption capacity and β is a constant related to the mean free energy of adsorption per mole of the adsorbate (mol^{2}J^{-2}), and ε is the polanyi potential. The constant, β gives an idea about the mean free energy E_s (kJ mol^{-1}) of adsorption per molecule of the adsorbate when it is transferred to the surface of the solid from infinity in the solution. C_e is the equilibrium concentration in the aqueous solution and q_e is the equilibrium adsorption capacity of adsorbent. The essential features of the isotherm can be expressed in terms of a dimensionless constant separation factor (R_L) that can be defined by the following relationship (Anirudhan and Radhakrishnan 2008):

$$R_L = \frac{1}{1 + K_L C_0} \tag{14}$$

According to both Table 3 and Fig. 12, the Langmuir isotherm model shows excellent fitness to the experimental data with high correlation coefficient at all temperatures. The maximum phenol adsorption capacity onto OPA is found to be 3.55 mgg^{-1} at 303 K.

The fitness of equilibrium data (Fig. 12) in Langmuir isotherm advocates the monolayer coverage of phenol onto OPA (Uddin et al. 2007). The essential features of Langmuir isotherm can be expressed in terms of a dimensionless constant separation factor (R_L). R_L value indicates the favorable adsorption of phenol onto OPA (Maheswari et al. 2009). Again from Table 4, it is clear that OPA is a good adsorbent for phenol among the other reported adsorbents. The Freundlich constant, K_F indicates the adsorption capacity of OPA and the value of K_F is 1.011 mgg^{-1}. Furthermore, the value of 'n' at equilibrium is 1.90, indicating favorable adsorption (Slejko 1985). From *D–R* isotherm the value of the adsorption energy is found to be 1.83 kJ mol^{-1} indicating the physisorption mechanism. Again from Temkin constants (B) which is related to the heat of adsorption is moderated. However, other equilibrium constant (K_T) data (5.69 L/mg) suggest the maximum binding energy between OPA and phenol molecules (Table 5).

Adsorption kinetic models

Kinetic models are used to evaluate the rate of the adsorption process and rate-controlling step. In the present communication, the kinetic data obtained from batch studies are analyzed using the following kinetic models (Table 6).

$$\text{Pseudo first} - \text{order}: \quad \log(q_e - q_t) = \log q_e - \frac{k_1 t}{2.303} \tag{15}$$

$$\text{Pseudo second} - \text{order}: \quad \frac{t}{q_t} = \frac{1}{k_2 q_e^2} + \frac{1}{q_e}t \tag{16}$$

The intra-particle diffusion:

$$q_e = k_{id}t^{0.5} + C \tag{17}$$

where q_e and q_t are concentrations of phenol at equilibrium and at time t. k_1 and k_2 are constants of the pseudo-first- and pseudo-second-order kinetic model. K_{id} is the constant of intra-particle diffusion model and C is related to boundary layer effect. The results of three kinetic models are shown in the Table 5 to find out the best fit rate of reaction for the adsorption of phenol onto OPA. According to linear regression correlation coefficients (Table 5), the rate of adsorption is found to follow the pseudo-second-

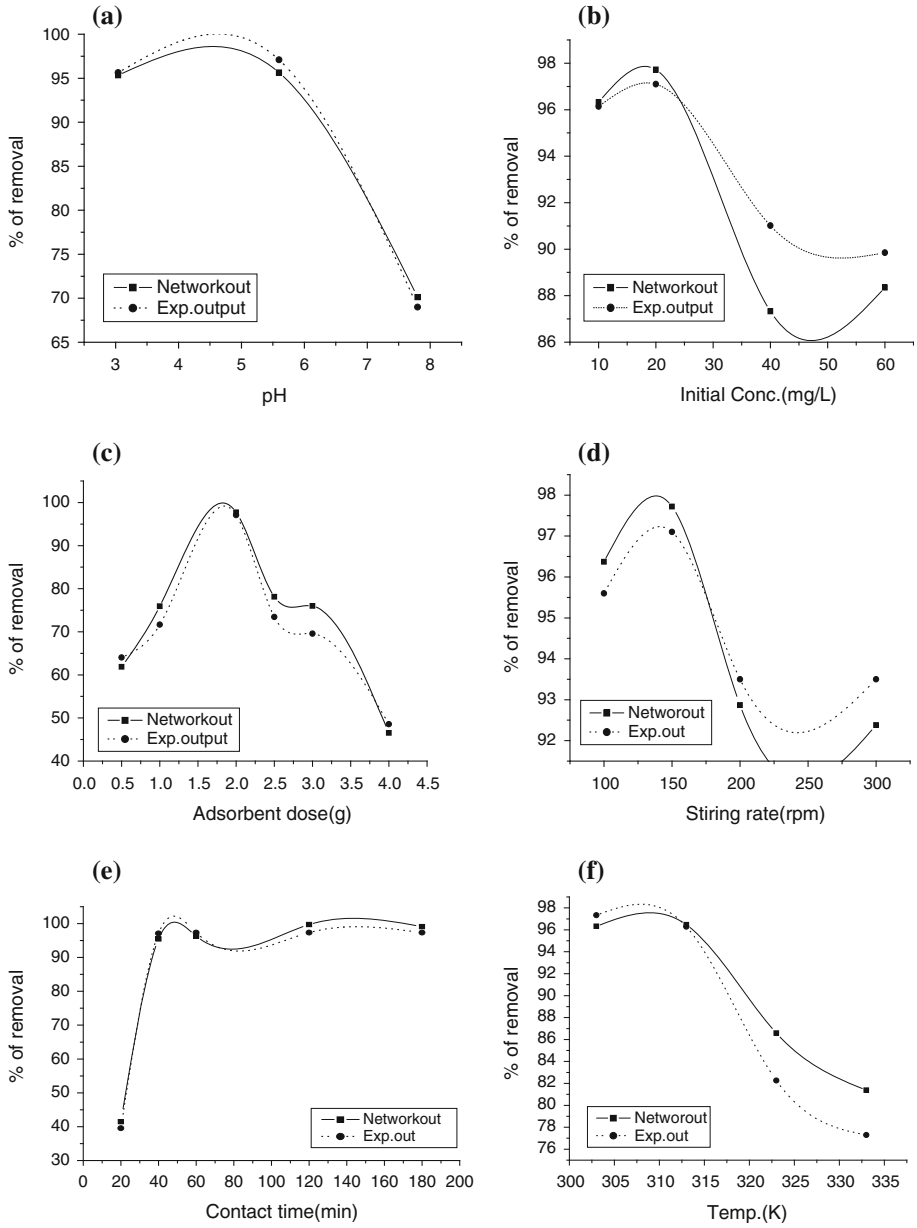

Fig. 11 Agreement between ANN outputs and experimental data as a function of **a** pH, **b** initial concentration (mg L^{-1}), **c** adsorbent dose, **d** stirring rate, **e** contact time (min) and **f** temperature (K)

Table 2 Equations of Isotherm models used in adsorption of phenol onto OPA

Isotherm models	Linear expression	Plot	Parameters	References
Langmuir	$\frac{1}{q_{eq}} = \frac{1}{q_{max} K_L C_e} + \frac{1}{q_{max}}$	$1/q_e$ vs. $1/C_e$	q_{max} = 1/intercept, K_L = 1/(slope × q_m)	Langmuir (1916)
Frreundlich	$\log q_{eq} = \log K_F + \frac{1}{n} \log C_e$	log (q_e) vs. log (C_e)	K_F = intercept, $1/n$ = slope	Freundlich (1906)
Temkin	$q_e = B \ln K_T + B \ln C_e$	q_e vs. ln C_e	B = slope, K_T = intercept	Wasewar et al. (2009)
DR	$\ln_{qe} = \ln_{qm} - \beta \varepsilon^2 E_s = \frac{1}{\sqrt{2\beta}}$	ln q_e vs. ε^2	β = slope, q_m = intercept	Kalavathy et al. (2010)

order kinetic model and the theoretical q_e value is closer to the experimental q_e value. In the view of the present results, it can be said that the pseudo-second-order kinetic model provides a good correlation for the adsorption of phenol onto OPA compared to that of pseudo-first-order model (Figs. 13, 14). Therefore, Pseudo-second-order model is highly applicable for this adsorption process. To identify the diffusion mechanism, the kinetic results are analyzed using the intra-particle diffusion model (Weber and Morris 1963).

Table 3 Adsorption isotherm constants for adsorption of phenol onto OPA

Parameters of adsorption isotherm models	Values
Langmuir	
q_m (mgg^{-1})	3.55
K_L	0.45
R^2	0.98
R_L	0.18
Freundlich	
K_F	1.01
$1/n$	0.52
R^2	0.91
D–R	
q_m (mgg^{-1})	7.22
B	0.15
E_s	1.83
R^2	0.95
Tempkin	
K_T	5.69
B	0.72
R^2	0.93

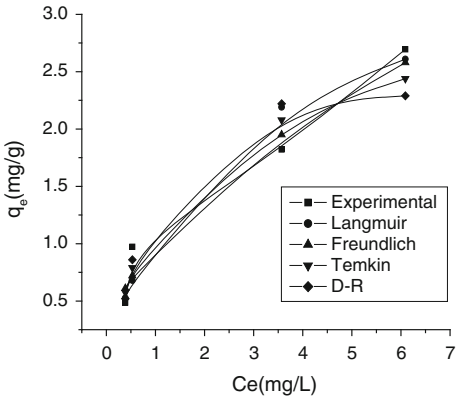

Fig. 12 Comparison between the measured and modeled isotherm profiles for the adsorption of phenol by orange peel ash (experimental conditions: Initial concentration 20.0 mg L^{-1}; pH—5.0; adsorbent dose 2.0 g; stirring rate 150 rpm; contact time 60 min, temperature 298 K)

Table 4 Maximum adsorption capacities, q_{max} (mg/g), for the adsorption of phenolic compounds by various adsorbents

Adsorbents	q_{max} (mg/g)	References
S. *muticum*	4.6	Rubin et al. (2006)
Lignite	10.0	Polat et al. (2006)
Rice husk	4.5	Ahmaruzzaman and Sharma (2005)
Chicken feathers	19.5	Banat and Al-Asheh (2000)
Bentonite	1.712	Banat et al. (2000)
Orange peel ash	3.55	Present study

Table 5 Kinetic model constants for adsorption of phenol onto OPA

Kinetic models		Experimental q_e
Pseudo-first-order	$q_e = 0.368$	0.973
	$K_1 = 0.006$	
	$R_1^2 = 0.316$	
Pseudo-second order	$q_e = 1.133$	
	$K_2 = 0.0374$	
	$R_2^2 = 0.9755$	
Intra-particle diffusion	$K_{id} = 0.002$	
	$C = 0.056$	
	$R^2 = 0.91$	

Thermodynamic parameters

The Gibbs free energy ($\Delta G°$) for the adsorption of phenol onto OPA is calculated following the equation ($\Delta G° = -\mathrm{RT} \ln K$) and data are presented in Table 7. The values for $\Delta H°$ and $\Delta S°$ are determined from the slope and intercept of the plot of $\Delta G°$ vs. T (figure not shown) and are also listed in Table 7. The negative value of $\Delta G°$ at all temperature indicates the feasibility as well as spontaneity of the phenol adsorption on OPA. Decrease in the value of $\Delta G°$ with increase in temperature suggests that lower temperature favors the adsorption (Saha et al. 2010). The negative value of $\Delta H°$ implies that the adsorption phenomenon is exothermic while the negative value of $\Delta S°$ suggests the process is enthalpy oriented (Saha et al. 2010).

Activation energy

The activation energy (E_a) usually provides important information on the mechanism of adsorption reaction. Using the pseudo-second-order rate constant, k_2 the activation energy, E_a for the adsorption of phenol on OPA is determined using the Arrhenius equation (18).

$$\ln k = \ln A - \frac{E_a}{\mathrm{RT}} \tag{18}$$

where k is the rate constant, A is the Arrhenius constant, E_a is the activation energy (kJ mol^{-1}), R is the gas constant (8.314 J mol^{-1}K^{-1}) and T is the temperature (K). By plotting $\ln k_2$ vs. $1/T$, E_a is obtained from the slope of the linear plot (Fig. 15). The activation energy is very significant to evaluate whether the entire adsorption reaction is physisorption or chemisorptions. If the value for activation energy lies between 8 and 16 kJ mol^{-1}, it is chemisorptions, and when it is below 8 kJ mol^{-1}, it is physisorption (Hai-jun et al. 2009). Here the E_a value is -18.001 kJ mol^{-1}. The measured E_a value suggests that the adsorption may be a physical adsorption.

Table 6 Equations of kinetic models used in adsorption of phenol onto OPA

Parameters	Linear form	References	Plot	Parameters
Kinetic models				
Pseudo-first-order	$\log(q_e - q_t) = \log q_e - \frac{k_1 t}{2.303}$	Theivarasu et al. 2011	$\log(q_e - q_t)$ vs. t	q_e = intercept, k_1 = (slope × 2.303)
Pseudo-second-order	$\frac{t}{q_t} = \frac{1}{k_2 q_e^2} + \frac{t}{q^e}$	Ho and Mc Kay (1998)	t/q_t vs. t	slope = $1/q_e$, intercept = $\frac{1}{k_2 q_e^2}$
Intra-particle diffusion model	$q = k_{id}\, t^{1/2} + C$	Weber and Morris (1962)	q vs. $t^{1/2}$	k_{id} = slope C = intercept

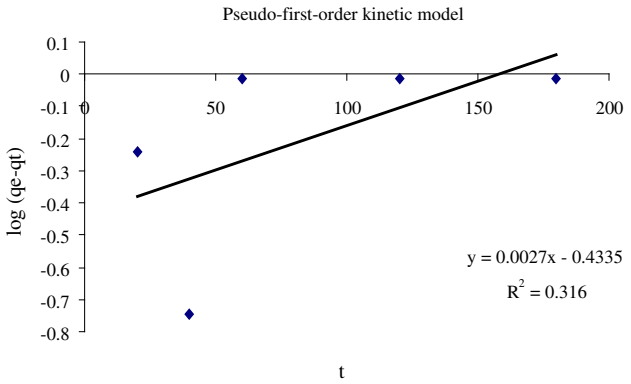

Fig. 13 Pseudo-first-order adsorption kinetic model for phenol adsorption with OPA

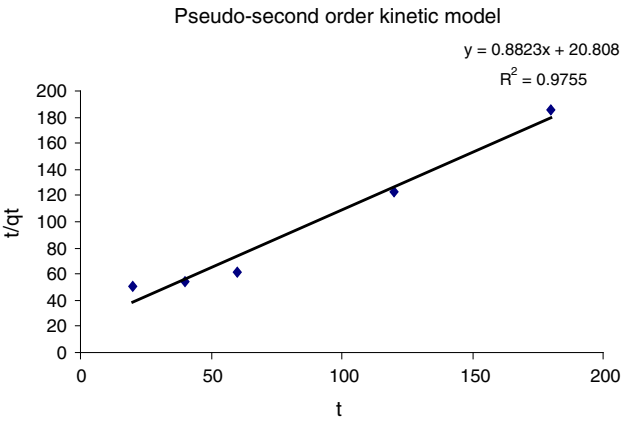

Fig. 14 Pseudo-second-order adsorption kinetic model for phenol adsorption with OPA

Tested with ANN model

The trained ANN model is tested and validated with the experimental results to estimate the phenol concentration. The network is trained with given input data set (Table 8). The training phase is completed after 6,00,000 epochs (Fig. 16). The lower value of MSE indicates the degrees of error that means network gives correct output. It is also clear from the Fig. 16 that with the increasing epoch the network is trained more accurately and subsequently more accurate and perfect output is achieved.

After the training phase the network shows optimum result describing the dynamics of phenol adsorption from aqueous solution. Finally in testing phase, the results show that the network output is matched with the experimental output (Fig. 11a–f). It is observed from Fig. 16 that MSE value is 0.0017 for one epoch that decreases with the increasing number of epochs and found minimum (0.0006) at 11 numbers of epochs. So the 11 number of hidden layer may be considered as optimum for this ANN model.

Table 7 Thermodynamic parameters for phenol adsorption onto OPA

$\Delta G°$ (kJ mol^{-1})				$\Delta H°$ (kJ mol^{-1})	$\Delta S°$ (kJ mol^{-1})
298	303	308	313	−85.09	−0.25
−9.1	−7.825	−6.55	−5.275		

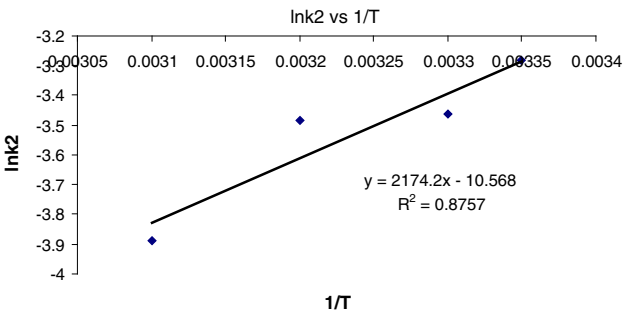

Fig. 15 Plot of $\ln k_2$ vs. $1/T$

Conclusion

It has been found that the OPA has enough potentiality to remove phenol from water. The operational parameters such as pH, initial phenol concentration, adsorbent dose, contact time, stirring rate and temperature have significant influence on the adsorption efficiency of OPA. The

Table 8 The outputs of MLP

Learning rate 0.001								
No. of iterations 600,000								
Testing phase Data	pH	Concentration	Dose	Time	Stirring rate	Temperature	Network output	Exp. output
Sigmoid function	5.6	20	0.5	40	150	303	60.26	64.05
	5.6	20	3	40	150	303	70.33	69.56
	5.6	60	2	40	150	303	87.67	89.85
Tanh function	5.6	20	0.5	40	150	303	62.18	64.05
	5.6	20	3	40	150	303	77.77	69.56
	5.6	60	2	40	150	303	88.44	89.85
TAN1.5H function	5.6	20	0.5	40	150	303	62.07	64.05
	5.6	20	3	40	150	303	77.38	69.56
	5.6	60	2	40	150	303	90.002	89.85

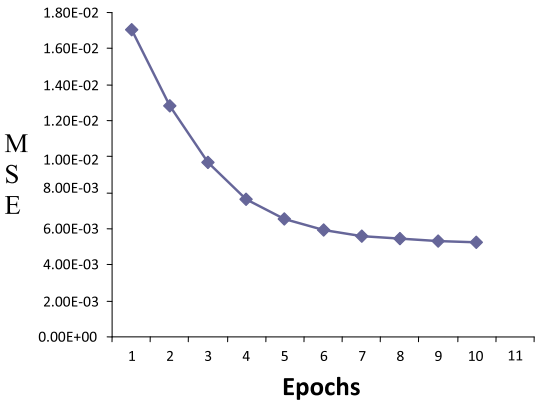

Fig. 16 Relation between the MSE and number of epochs

maximum adsorption capacity is 3.55 mgg^{-1} at 20 mg L^{-1} initial phenol concentration. The multi-layer ANN modeling technique can be applied to optimize the process. The Back Propagation Algorithm (BPA) is found to be the best algorithm with a minimum mean squared error (MSE) for training 0.00528. The temperature has strong influence on the adsorption process and the maximum removal is observed at 298 K. The kinetic study reveals that the adsorption process usually follows pseudo-second order. Langmuir isotherm model is in accordance with the experimental data. Moreover, thermodynamic parameters are in favor of exothermic and spontaneous nature of adsorption of phenol onto OPA.

Acknowledgments The authors are grateful to Dr. Alak Kumar Ghosh, Associate Professor, Department of Chemistry, Burdwan University, Burdwan, West Bengal, India for recording FTIR data. The authors would like to extend their gratitude to Dr Srikanta Chakraborty, In charge of SEM, USIC, University of Burdwan, West Bengal, India for SEM study.

References

Ademiluy FT, Amsfi SA, Amakama NJ (2009) Adsorption and Treatment of organic contaminants using activated carbon from waste Nigerian Bamboo. J Appl Sci Environ Manage 13:39–47

Ahmaruzzaman M, Sharma DK (2005) Adsorption of phenol from waste. Water J Colloid Interface Sci 287(1):14–24

Aksu Z, Yener J (2001) A comparative adsorption/biosorption study of monochlorinated Phenols onto various sorbent. Waste Manag 21:695–702

Anirudhan TS, Radhakrishnan PG (2008) Thermodynamics and kinetics adsorption of Cu (II) from aqueous solution on to a new cation exchanger derived from tamarind fruit shell. J Chem Thermodyn 40:702–709

APHA, AWWA, WEF (1995) Standard methods for the examination of water and Wastewater, 19th edn. Washington

Asma S, Zainal A (2009) Adsorption of phenol by activated carbon produced from decanter cake, Eng D thesis, University Malaysia Pahan

Banat FA, Al-Asheh S (2000) Biosorption of phenol by chicken feather. Environ Eng Policy 2(2):85–90

Banat FA, Al-Bashir B, Al-Asheh S, Hayajneh O (2000) Adsorption of phenol by bentonite. Environ Pollut 107:391–398

Bhattacharjya RK, Datta B, Satish MG (2007) Artificial neural networks approximation of density dependent saltwater intrusion process in coastal aquifers. J Hydrol Eng 12(3):273–282

Bhatti HN, Nasir AW, Hanif MA (2010) Efficacy of Daucus Carotal Waste biomass for the removal of chromium from the aqueous solution. Desalination 253:78–87

Carsky M, Do DD (1999) Neural network modeling of adsorption of binary vapour mixtures. Adsorption 5:183–192

Caturla F, Martin-Martinez JM, Molina-Sabio M, Rodrignez-Reinoso F, Torregrosa R (1998) Adsorption of substituted phenols on activated carbon. J Colloid Interface Sci 124:528–534

Chelani AB, Chalapati Rao CV, Phadke KM, Hasan MZ (2004) Prediction of sulphur dioxide concentration using artificial neural networks. Environ Model Softw 17:161–168

Cuco APC, Neto AJS, Velho HFC, Sousa FL (2009) Solution of an inverse adsorption problem with an epidemic genetic algorithm and the generalized extremal optimization algorithm. Inverse Prob Sci Eng 17:289–302

Eahart JP, Won K, Wang HY, Prausnitz JM (1977) Recovery of organic pollutants via solvent extraction. Chem Eng Prog 73:67–73

Freundlich H (1906) Over the adsorption in solution. Z Phys Chem 57:385–470

Gholami F, Mahvi AH, Omrani GhA, Nazmara Sh, Ghasri A (2006) Removal of Chromium from aqueous solution. Iran J Environ Health Sci and Eng 3:97–102

Hai-jun L, Mao-tian L, Jin-li Z (2009) A kinetic study on the Adsorption of Chromium (VI) onto a natural Material used as Landfill Liner. E J Geotech Eng 14:1–10

Hamza HA, Atieh MA, Laoui T (2012) Removal of phenol by carbon nanotubes and activated carbon—a comparative analysis, sixteen international water technology conference, IWTC, 16, Istanbul, Turkey

Hegazy AK, Abdel-Ghani NT, El-Vhaghaby GA (2013) Adsorption of phenol onto activated carbon from Rhazya stricta: determination of the optimal experimental parameters using factorial design. Appl Water Sci. doi:10.1007/s13201-013-0143-9

Ho YS, McKay G (1998) Kinetic model for lead (II) sorption onto peat. Ads Sci Technol 16:943–955

Imagawa A, Seto R, Nagaosa Y (2000) Adsorption of chlorinated hydrocarbons from air and aqueous solutions by carbonized rice husk. Carbon 38:623–641

Kalavathy H, Karthik B, Miranda LR (2010) Removal and recovery of Ni and Zn from aqueous solution using activated carbon from *Hevea brasiliensis*: batch and column studies. Colloid Surf B: Biointerface 78:291–302

Langmuir I (1916) The constitution and fundamental properties of solids and Liquids. J Am Chem Soc 38:2221–2295

Li XM, Tang YR, Xuan ZX, Liu YH, Luo F (2007) Study on the preparation of orange peel cellulose adsorbents and biosorption of Cd^{2+} from aqueous solution. Sep Purif Technol 55(1):69e75

Lotfy HR, Misihairabgwi J, Mutwa MM (2012) The preparation of activated carbon from aqroforestry waste for waste water treatment. Afr J Pure Appl Chem 6:149–156

Maheswari P, Venilamani N, Madhavakrishnan S, Sayed Sahabudeen PS, Nadavala SK, Veera MB (2009) Biosorption of phenolic compounds by Trametes versicolor polyporus Fungus. Adsorpt Sci Technol 27:231–237

Mehrizad A, Aghaie M, Gharbani P, Dastmatch S, Monajjemi M, Zare K (2009) Comparison of 4-Chloro-2-nitrophenol adsorption on single walled and multi-walled carbon nanotubes. Iran J Environ Health Sci Eng 9:5. doi:10.1186/1735-2746-9-5

Ning-chuan F, Xue-yi G (2012) Characterization of adsorptive capacity and mechanisms on adsorption of copper, lead and zinc by modified orange peel. Trans Nonferrous Met Soc China 22:1224–1231

Ogwueleka TCh, Ogwueleka FN (2010) Modelling energy content of municipal solid waste using artificial neural network. Iran J Environ Health Sci Eng 7:259–266

Olafadehan OA, Jinadu OW, Safami L, Popoola OT (2012) Treatment of Brewery waste water effluent using activated carbon prepared from coconut shell. Inter J Appl Sc Technol 2:165–178

Polat H, Molva M, Polat M (2006) Capacity and mechanism of phenol adsorption on lignite. Int J Miner Process 79:264–273

Rengaraj S, Seuny-Hyeon M, Sivabalan R (2002) Agricultural solid waste for the removal of organics: adsorption of phenol from water and wastewater by Palm seed coat activated carbon. Waste Manage 22:543–548

Rubin E, Rodriguez P, Herrero R, de Sastre Vicente ME (2006) Biosorption of phenolic compounds by the brown alga sargassum muticum. J Chem Technol Biotechnol 81:1093–1099

Saha P, Chowdhury S, Gupta S, Kumar I (2010) Insight into adsorption equilibrium, kinetics and thermodynamics of Malachite Green onto clayey soil of Indian Origin. Chem Eng J 165:874–882

Shan W, Fang D, Zhao Z, Shuang Y, Ning L, Xing Z, Xiong Y (2012) Application of orange peel for adsorption separation of molybdenum(VI) from Re-containing industrial effluent. Biomass Bioenergy 37:289–297

Slejko F (1985) Adsorption technology a step by step approach to process evaluation and application. Marcel Decker, New York, p 13

Theivarasu C, Mylsamy S, Sivakumar N (2011) Cocoa shell as adsorbent for the removal of methylene blue from aqueous solution: kinetic and equilibrium study. Univers J Environ Res Technol 1:70–78

Uddin MT, Islam MS, Abedin MZ (2007) Adsorption of phenol from aqueous solution by water hyacinth ash. ARPN J Eng Appl Sci 2:11–17

Wasewar KL, Kumar S, Prasad B (2009) Adsorption of tin using granular activated carbon. J Environ Prot Sci 3:41–52

Weber WJ, Morris JC (1962) Advances in water pollution research: Removal of biologically resitant pollutants from waste water by adsorption. In: Proceeding of international conference on water pollution symposium, vol 2, pp 231–266

Weber WJ, Morris JC (1963) Kinetics of adsorption on carbon from solution. J Sanit Eng Div Am Soc Civil Eng 89:31–39

WHO (2008) Guidelines for Drinking Water Quality: Incorporating First and Second Addenda. 3rd edn. vol 1. World Health Organization, Geneva

Zeng X, Fan Y, Wu G, Wang C, Shi R (2009) Enhanced adsorption of phenol from water by a novel polar post-crosslinked polymeric adsorbent. J Hazard Mater 169:1022–1028